CHEMIJA. 2017. Vol. 28. No. 4. P. 183–192

Performance of bis-[triethoxysilylpropyl] tetrasulfide silane coatings for improved corrosion resistance of carbon steel

O. Girčienė*,

L. Gudavičiūtė,

A. Martušienė,

A. Selskis,

V. Jasulaitienė,

R. Ramanauskas

Institute of Chemistry,
Center for Physical Sciences and Technology,
Saulėtekio Ave. 3, 10257 Vilnius, Lithuania

This work was aimed at evaluation of the effect of sol–gel coating of bis-[triethoxysilylpropyl] tetrasulfide (BTESPT) on improved corrosion resistance of carbon steel samples in a 0.5 M NaCl solution. The samples of carbon steel and phosphated carbon steel without/with cerium conversion films coated with BTESPT or BTESPT doped with cerium, as a corrosion inhibitor, were investigated. The composition and structure of the samples were characterised by the scanning electron microscope (SEM) and the X-ray photoelectron spectroscopy (XPS) techniques, while their corrosion behaviour was investigated applying voltametric and electrochemical impedance spectroscopy (EIS) measurements. The data obtained have shown that all phosphated carbon steel samples (without/with cerium conversion films) with the sol–gel coatings exhibited better protective abilities with respect to those of carbon steel. The results of EIS measurements revealed that the cerium conversion coatings or the addition of cerium nitrate, as an inhibiting agent, to BTESPT can certainly help in corrosion protection of carbon steel substrates. The film of BTESPT doped with Ce is more protective than that of non-modified ones.

Keywords: phosphated carbon steel, sol–gel coating, corrosion inhibitor, cerium

INTRODUCTION

Carbon steel is widely used in industry, however, its susceptibility to corrosion in many environments limits its applications. For many years, the best known industrial system used to improve corrosion resistance of metals has been established on chromate based coatings. These coatings have unrivalled self-healing abilities, which are believed to arise from the migration of a soluble Cr(VI) compound in the coating to a scratch or defect, where they are reduced to form a new protection layer [1, 2]. However, the chromate conversion coatings contain toxic and carcinogenic hexavalent chromium, so much research is directed to replacing it with more environment-friendly alternatives, such as phosphate conversion coatings [3–6], molybdate [7, 8], phosphate-permanganate [9, 10], rare-earth and other base materials [11–25].

* Corresponding author. Email: olga.girciene@ftmc.lt

The application of hybrid organic-inorganic sol–gel coatings on different substrates has been thoroughly investigated in recent years [26–31]. A sol–gel coating can be applied to a metal substrate through various techniques, such as dip-coating and spin-coating, which are the two most commonly used coating methods. Besides the resistance to corrosion, the sol–gel coatings can also provide high oxidation, abrasion, water resistance, and many other useful properties [26]. The silane coating is a passive organic coating [30], since it acts essentially as a physical barrier that hinders the penetration of aggressive species towards the metallic substrate. However, this behaviour can be modified through the inclusion of small amounts of a chemical possessing corrosion inhibiting properties.

The interest for use of the rare-earth compounds has been growing over the past 20 years. It has been demonstrated that they promoted protection to a significant number of metals and alloys, for example, steel, hot deep

galvanized steel, tin, aluminium and their alloys, etc. [11–25]. It has been reported that rare-earth ions such as Ce, La, etc. provide exceptional resistance to localised corrosion through the formation of insoluble hydroxide/oxide layers [24, 25]. A number of studies demonstrate that the cerium-based conversion coatings, in particular, could be considered as one of more promising chromate coatings substitutes, as the cerium compound does not present environmental problems and the coatings provide an efficient corrosion protection close to that of chromium [20, 23]. The incorporation of inhibitors into the sol–gel matrix is the simplest way of improving the protective properties against corrosion. Many inorganic inhibitors such as cerium salts, vanadates, molybdates, permanganates and phosphates have, therefore, been combined with various silane-based coatings in an attempt to substitute chromate-based pretreatments.

This work was aimed to evaluate the effect of sol–gel coatings of bis-[triethoxysilylpropyl] tetrasulfide (BTESPT) on improved corrosion resistance of carbon steel samples in a 0.5 M NaCl solution. The samples of carbon steel (CS) and phosphated carbon steel (FeP) without/with cerium conversion films coated with BTESPT (B) or BTESPT doped with $Ce(NO_3)_3$ (BCe), as a corrosion inhibitor, were investigated. The composition and structure of samples were characterized by the scanning electron microscopy and X-ray photoelectron spectroscopy techniques, the silane coatings were assessed for their corrosion behaviour using voltametric measurements and the electrochemical impedance spectroscopy (EIS) technique.

EXPERIMENTAL

Materials and sample preparation

Test specimens (10 × 20 × 1 mm) with an area of 4 cm^2 were prepared from carbon steel (CS) of the composition (wt. %): C 0.21%, Mn 1.2%, Si 0.6%, Cr ≤ 0.3%, Ni < 0.3%, Cu < 0.3%. P < 0.4%, S < 0.045%. The samples were previously polished with emery paper up to grade 400, degreased with ethanol and rinsed with distilled water.

The phosphating solution was used for the formation of an amorphous phosphate coating (FeP): 0.15 M H_3PO_4, 0.003 M $H_2C_2O_4$, pH = 4–5, 50°C, 10 min. Cerium conversion coatings Ce1 and Ce2 were formed by a simple immersion of the samples for 24 h at 25°C into solutions containing 0.05 M $Ce(NO_3)_3$ and 0.05 M $Ce(NO_3)_3$ + 0.025 M Na_2SO_4, respectively.

The solution for the sol–gel coating B was prepared by dissolving 4% (v/v) of BTESPT in a mixture of ethanol (90.5% v/v) and deionized water (5.5% v/v). The solution for the sol–gel coating doped with cerium BCe was prepared by dissolving 4% (v/v) of BTESPT in a mixture of ethanol (90.5% v/v) and an aqueous solution of 0.001 M $Ce(NO_3)_3$ (5.5%, v/v). The solutions were stirred for one hour and stored for 3 days before being used for the pre-treatment of the investigated samples. The samples were immersed into the solution B or BCe for 10 s and cured at 120°C for 40 min [27].

The investigated multilayer coatings systems consisted of a FeP layer, two types of cerium conversion coatings Ce1, Ce2 and, additionally, an outer layer of BTESPT or BTESPT doped with cerium.

Morphology and composition

The microstructure and elemental composition of specimens were studied by a scanning electron microscope (SEM). A Helios NanoLab 650 dual beam workstation (FEI) with an X-Max 20 mm^2 energy dispersive detector (energy resolution of 127 eV for Mn Ka, Oxford Instruments) was used for imaging and energy dispersive analysis. The deposited film thickness analysis was performed on the produced and vacuum Pt coated cross-sections of the samples by the focused ion beam (FIB) technique.

X-ray photoelectron spectroscopy (XPS) studies were performed by a spectrometer ESCALAB using X-radiation of MgK_α (1253.6 eV, pass energy of 20 eV). To obtain depth profiles, the samples were etched in a preparation chamber by ionised argon at a vacuum of 5×10^{-4} Pa. an accelerating voltage of ca. 1.0 kV and a beam current of 20 μA cm^{-2} were used.

Electrochemical measurements

The corrosion behaviour of samples was investigated in an aerated stagnant 0.5 M NaCl solution. The electrolyte was prepared from analytical grade chemicals and deionized water. All electrochemical measurements were performed at ambient temperature with an Autolab PGSTAT302 potentiostat using a standard three-electrode system with a Pt counter electrode and a saturated Ag/AgCl reference electrode. All potentials are reported versus the saturated Ag/AgCl reference electrode. The corrosion current densities (i_{corr}) were determined from voltammetric measurements by Tafel line extrapolation. A specimen was polarized with a potential scan rate of 0.5 mV s^{-1}, from the cathodic to the anodic region. The polarization resistance (R_p) values were determined from linear polarization measurements, which were performed between ±10 mV around E_{corr}, after immersion into the solution for 1 h, with a scan rate of 0.1 mV s^{-1}.

The measurements of electrochemical impedance spectra (EIS) were performed at the open circuit potential with the FRA2 module applying a signal of 10 mV amplitude in the frequency range 20 kHz to 0.001 Hz. The data obtained were fitted and analysed using the EQUIVCRT program of Boukamp [32].

Electrochemical experiments were performed at least in duplicate samples.

RESULTS AND DISCUSSION

Morphology and composition

The sol–gel coating of BTESPT was chosen for steel corrosion prevention investigations because it forms films with a very high hydrophobic performance and therefore good potentialities for corrosion protection [33]. One of the main problems

when applying sol–gel coatings on iron based alloys is the lack of adherence of the film formed on a substrate that easily oxidizes forming bulky oxides as Fe_2O_3 [29]. Therefore the phosphate conversion treatment was applied prior to silane coatings deposition. Amorphous phosphate coating FeP was formed in the solution which did not contain any other constituent metal ions but only the acid phosphates of potassium. A compact layer of *ca*. 200 nm in thickness consists of a mixture of iron phosphate and iron oxide and is generally regarded as being amorphous, and the detailed studies on this object are presented in [33]. However, all the mentioned coatings offer only passive corrosion protection, therefore, the addition of corrosion inhibitors, with the aim to impart active corrosion protective properties to the coatings, is of great interest. The role of corrosion inhibitors in these multilayer coating systems was assigned to cerium compounds. In order to determine the most effective application of this inhibitor, the investigated CS and FeP samples were coated with cerium conversion coatings Ce1 or Ce2 and additionally with either a layer of silane (CSCe1/B, CSCe2/B and FePCe1/B, FePCe2/B) or a layer of silane doped with cerium (CS/BCe, FeP/BCe).

SEM images of the surface morphology and cross-sections of the most representative investigated samples FeP/B, FeP/BCe, FePCe1/B and FePCe2/B are presented in Fig. 1. All

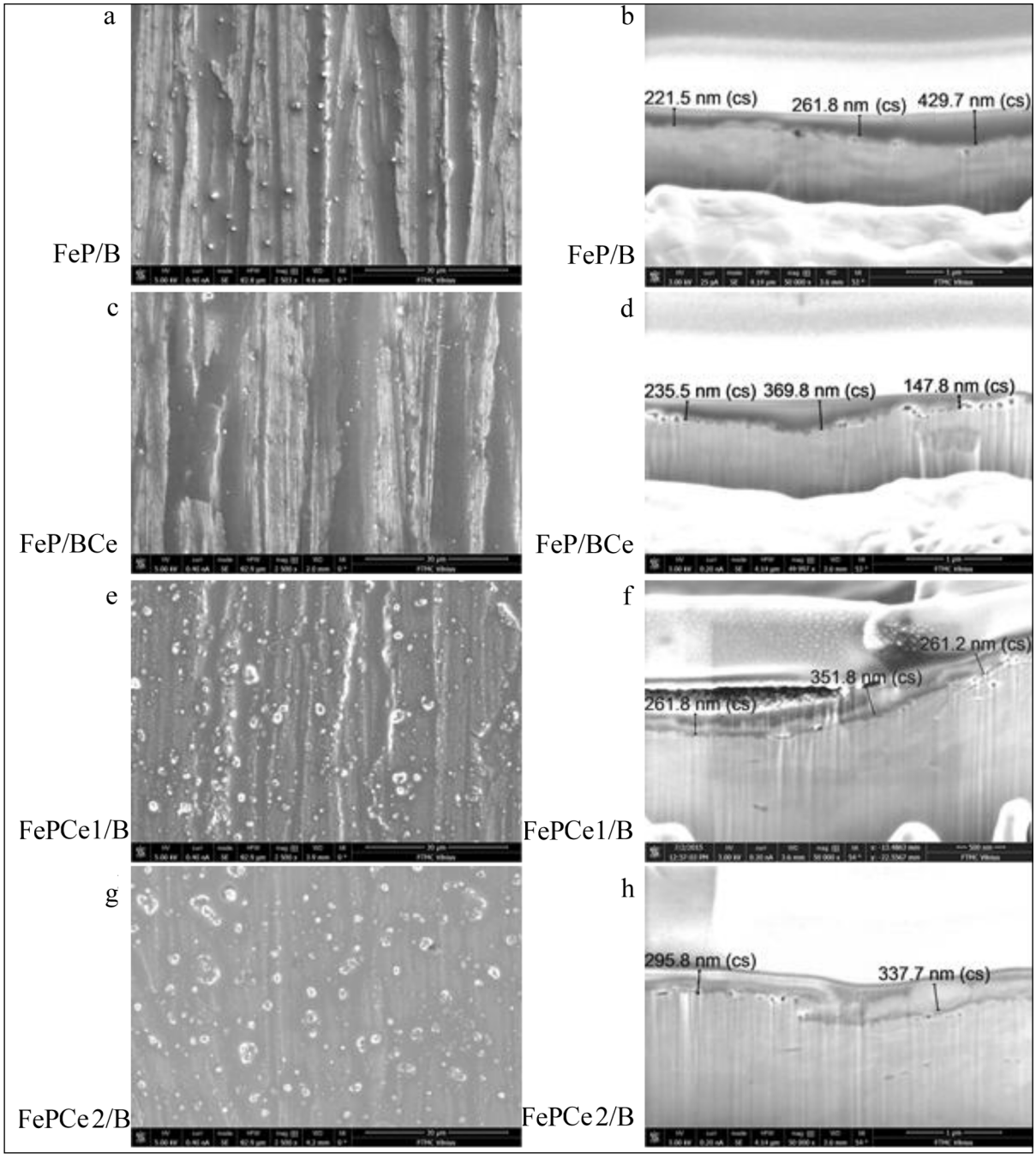

Fig. 1. SEM images of the microstructure (a, c, e, g) and the cross-section (b, d, f, h) of FeP/B (a, b), FeP/BCe (c, d), FePCe1/B (e, f), FePCe2/B (g, h) samples

the formed BTESPT coatings in the multilayer coating systems are free of visible defects and cracks (Fig. 1a, c, e, g). While the phosphate layer thickness is ~200 nm, the overall average thickness of the multilayer coatings varied between 250 and 320 nm. The values of the average thickness of BTESPT coatings on the FeP surface (without/with Ce1 and Ce2 films) did not differ much from each other, as they were 305 and 316 nm, respectively (Fig. 1 b, f, h). Meanwhile, the introduction of Ce into the sol–gel coating led to the reduction of the resulting film thickness up to ~250 nm (Fig. 1d).

The analysis of the elemental composition of investigated samples FeP/B, FeP/BCe, FePCe1/B and FePCe2/B was performed by EDS measurements, the results of which are listed in Table 1. The data obtained indicate that the most intensive signal was observed from the base metal Fe (Table 1), while another dominant element in the films is O. The fact that the amount of P both in a pure phosphate film and that one modified with Ce was close to 1 at.% implies that Fe oxides are one of the principal constituents of the formed conversion films. The amount of Ce in the multilayer coatings varied from 0.2 to 2.4 at.% and it was detected to be higher for FeP samples with conversion coatings of cerium and especially for FePCe2/B. The amount of Ce in the multilayer coating was the lowest one (~0.2 at.%) when Ce was doped directly into the silane sublayer FeP/BCe. Besides, all silane-coated samples contained ~2.2–3.6 at.% of Si and 2.7 to 5.5 at.% of S. These elements are the constituent parts of BTESPT.

Table 1. **The elemental composition of the FeP samples treated with silane BTESPT (B) and with BTESPT doped with cerium (BCe)**

Sample	Elements, at.% (by EDS)					
	O	Si	P	S	Fe	Ce
FeP/B	20.1	2.2	1.0	2.7	74.0	–
FeP/BCe	20.9	3.6	1.0	4.4	69.9	0.2
FePCe1/B	30.8	2.7	0.9	3.2	61.5	0.9
FePCe2/B	40.5	2.9	0.8	5.5	47.9	2.4

The composition and the oxidation state of elements in the outer part of the sol–gel coating of BCe on CS and FeP were examined using XPS measurements. O 1s, Fe $2p_{3/2}$, Ce 3d, P 2p, Si 2p spectra were recorded after surface sputtering with Ar^+ ions for an increasing period of time. The surface layer composition was determined and the results are listed in Table 2. In general, according to the XPS measurements, the top layer (0–20 nm depth) of the samples seems to be rich in C, S, O and Si. O 1s spectra of the samples exhibited a peak at 533.53–534.75 eV, which may be assigned to SiO_2, and Si 2p spectra exhibited a peak at 103.32–104.43 eV also indicating SiO_2. The Ce 3d spectra for the FeP/BCe sample are presented in Fig. 2. The peaks for the Ce 3d region in the binding energy range from 880 to 920 eV were not detected, while the calculated amount of Ce in the coatings varied from 0.16 to 0.4 at.% (Table 2).

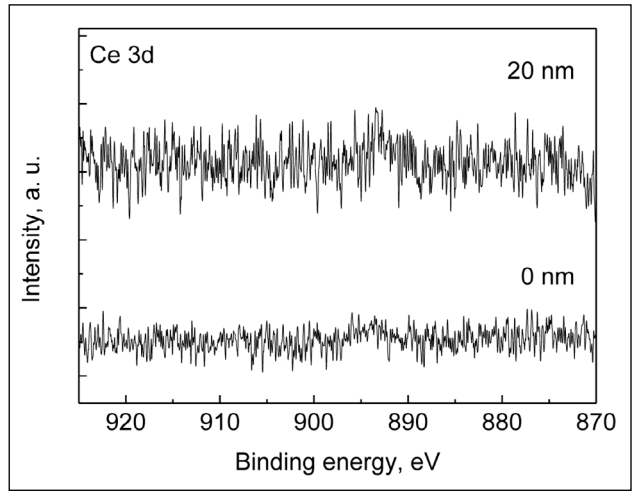

Fig. 2. XPS spectra for the Ce 3d region obtained on the FeP/BCe sample at different sputtering times

Evaluation of corrosion resistance

Potentiodynamic polarization measurements

The corrosion behaviour of CS and FeP samples with multilayer coating systems (without/with Ce1 or Ce2 conversion coatings and with B or BCe layers) was investigated by linear polarization measurements, which were carried out in a 0.5 M NaCl solution. The potentiodynamic polarization curves of the investigated samples are shown in Figs. 3 and 4. The data

Table 2. **XPS analysis data of the CS and FeP samples treated with BCe**

Sample	Elements, at.%								
	Si	P	S	Mo	C	N	O	Fe	Ce
0 nm depth									
CS/BCe	15.57	–	18.39	–	41.82	–	22.94	1.05	0.24
FeP/BCe	15.58	–	15.15	–	46.12	–	23.00	–	0.16
20 nm depth									
CS/BCe	25.81	–	21.74	0.22	16.16	3.22	31.91	1.63	0.31
FeP/BCe	26.02	1.49	20.41	0.22	20.78	4.72	24.89	1.08	0.4

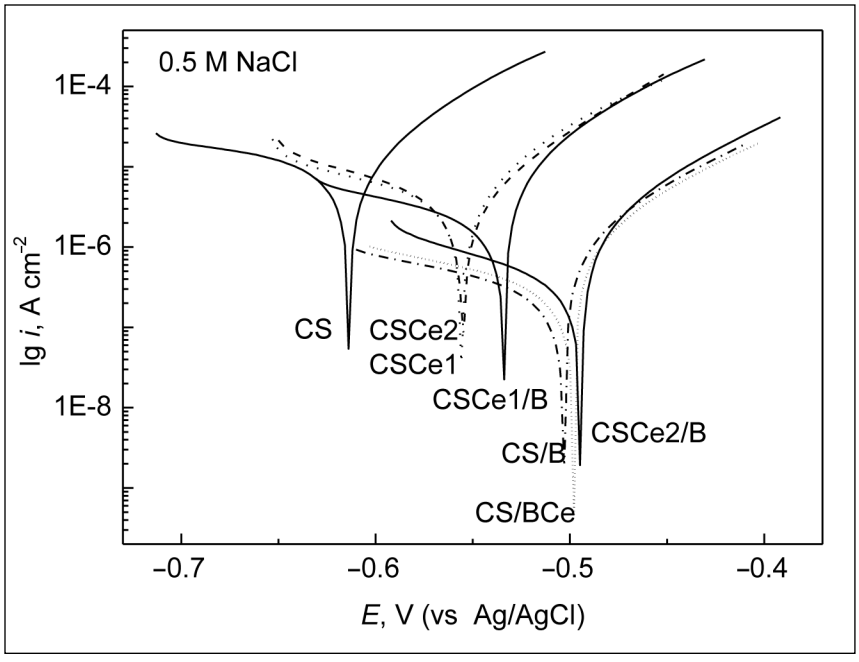

Fig. 3. Potentiodynamic polarization curves of the CS samples measured in a 0.5 M NaCl solution at 25°C, 0.5 mV s^{-1}

obtained have shown that the corrosion potential E_{corr} of all samples treated with B and BCe exhibited more positive E_{corr} values as compared to those without silane layers (Fig. 4). It is evident that the samples of FeP with silane layers exhibited ~50–100 mV more positive E_{corr} values, with respect to the samples with a silane layer deposited directly on the CS surface. The values of i_{corr} were determined from the Tafel line extrapolation and the results obtained are listed in Table 3. As seen from the data, the samples of CS and FeP with conversion coatings Ce1, Ce2 and treated with B exhibited the lowest values of i_{corr}, which varied in the range of $2.5 \cdot 10^{-7}$–$8.8 \cdot 10^{-8}$ A cm^{-2}. The protection efficiency *P*% of the investigated samples was calculated by the equation [13, 14]

$$P\% = (i^{o}_{corr} - i_{corr})/i^{o}_{corr} \times 100, \quad (1)$$

where i^{o}_{corr} and i_{corr} denote the corrosion current density of the electrode without [33] and with B or BCe coatings (Table 3), respectively. The results obtained imply that all the investigated samples treated with sol–gel coatings demonstrated better protective properties after 0.5 h exposure to a 0.5 M NaCl solution. The calculated values of *P*% increased from 80% up to 95% and the highest *P*% value was stated for the FePCe2/B sample (Table 3).

The values of R_p of the investigated samples, which were determined from the linear polarization measurements ±10 mV around E_{corr}, are listed in Table 3. It is evident that

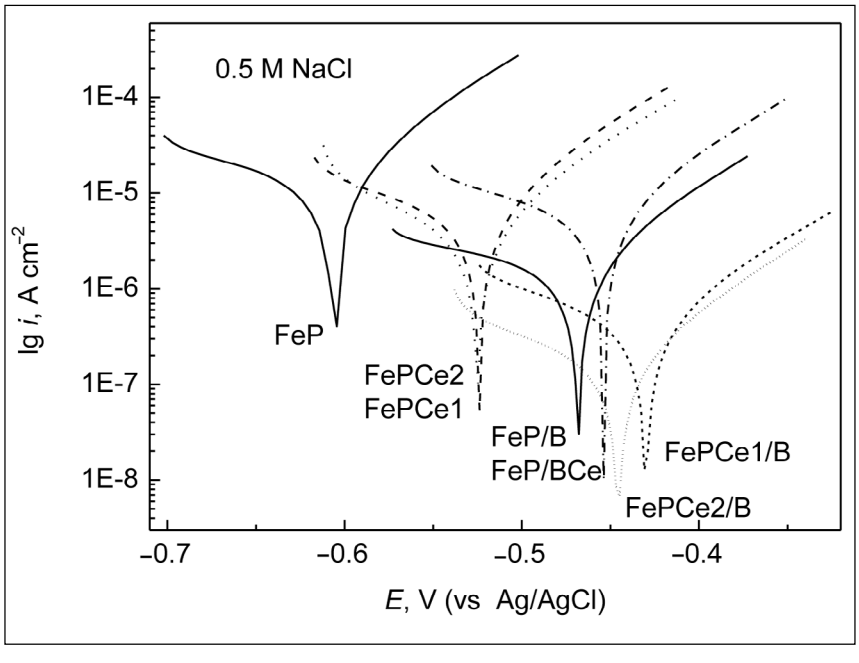

Fig. 4. Potentiodynamic polarization curves of the FeP samples measured in a 0.5 M NaCl solution at 25°C, 0.5 mV s^{-1}

Table 3. **The electrochemical parameters (corrosion potential E_{corr}, corrosion current density i_{corr}, polarization resistance R_p) and the protection efficiency P% of the investigated samples determined in a 0.5 M NaCl solution**

Sample	Electrochemical parameters			
	E_{corr}, V (vs Ag/AgCl)	i_{corr}, A cm^{-2}	P%	R_p, kΩ cm^2 (±10 mV)
CS*	–0.609	$5.3 \cdot 10^{-6}$	–	0.95
CS/B	–0.503	$8.9 \cdot 10^{-7}$	83	9.2
CS/BCe	–0.498	$6.3 \cdot 10^{-7}$	88	10.5
CSCe1*	–0.556	$1.6 \cdot 10^{-6}$	–	3.31
CSCe1/B	–0.531	$2.5 \cdot 10^{-7}$	84	26.3
CSCe2*	–0.555	$1.7 \cdot 10^{-6}$	–	2.2
CSCe2/B	–0.494	$1.9 \cdot 10^{-7}$	89	27.5
FeP*	–0.588	$3.1 \cdot 10^{-6}$	–	1.65
FeP/B	–0.468	$6.2 \cdot 10^{-7}$	80	25.5
FeP/BCe	–0.455	$5.4 \cdot 10^{-7}$	83	40.6
FePCe1*	–0.525	$1.4 \cdot 10^{-6}$	–	3.53
FePCe1/B	–0.430	$2.3 \cdot 10^{-7}$	84	60.5
FePCe2*	–0.524	$1.6 \cdot 10^{-6}$	–	2.94
FePCe2/B	–0.445	$8.8 \cdot 10^{-8}$	95	79.5

* O. Girčienė, L. Gudavičiūtė et al. [33].

all FeP (without/with Ce1, Ce2) samples additionally coated with B or BCe exhibited up to threefold higher R_p values, as compared with those of CS, respectively. The FePCe1/B and FePCe2/B samples exhibited the highest values of R_p (Table 3). It can be stated, therefore, that the FeP samples with the multilayer coatings (FeP/B, FeP/BCe, FePCe1/B, FePCe2/B) exhibited better protective abilities with respect to those of the CS samples.

EIS investigation

Sol–gel coatings, used as protection against metal corrosion, do not usually improve their protection ability with the increase of contact with the aggressive media time. In fact, depending on the composition and structure of the coating, deterioration of the coating may occur, permitting the contact of electrolyte with the substrate and thus decreasing the protective effect [30, 31]. The EIS technique can give important information on the kinetics of evolution of the coating degradation and the corrosion activity during its immersion into the corrosive media.

The EIS diagrams of the samples of FeP with the multilayer coatings after 0.5 h exposure to a 0.5 M NaCl solution are presented in Fig. 5. In general, the EIS spectra of the FeP/B and FeP/BCe samples and those of the FePCe1/B and FePCe2/B samples show two similar features. Two different electrical circuits were used to fit the experimental data (Fig. 6a, b). The selected models have been widely used for the analysis of the impedance spectra of sol–gel coated metals [34, 35]. The circuit shown in Fig. 6a was used to

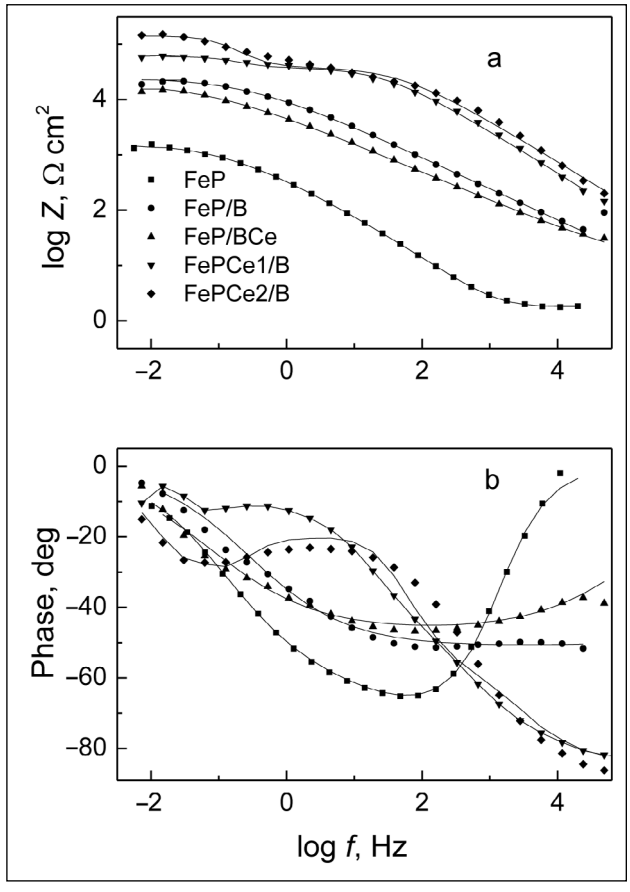

Fig. 5. Bode plots of EIS spectra after immersion of samples in a 0.5 M NaCl solution for 0.5 h

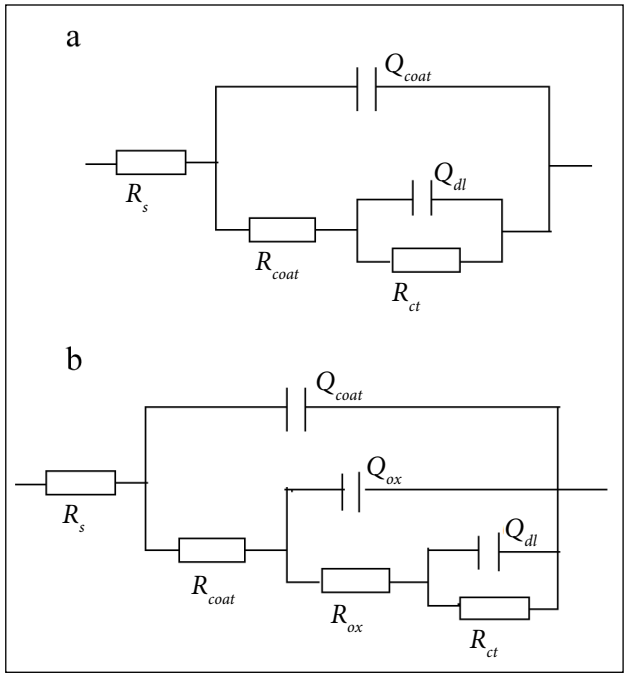

Fig. 6. Equivalent circuit models used for EIS data fitting

fit the experimental data of the FeP samples coated with B and BCe, whose impedance magnitude $|Z|$ shows two well-defined time constants (Fig. 5). The region between 10^2 and 10^5 Hz provides information on the sol–gel coating pore resistance (R_{coat}) and capacitance (C_{coat}). The low frequency region provides information on the corrosion process characterized by the charge transfer resistance (R_{ct}) and double layer capacitance (C_{dl}). The FeP samples coated with the Ce1 and Ce2 conversion coatings and additionally with a B film show three well-defined time constants (Fig. 5). In this case the third time constant corresponding to the contribution from the intermediate cerium oxide layer mainly appears at frequencies lower than 10^2 Hz. More detailed information on the cerium oxide layer resistance (R_{ox}) and capacitance (C_{ox}) can be extracted from the fitting of the EIS spectra using the equivalent circuit presented in Fig. 6b.

For fitting the data, all the capacitances in the equivalent circuits had to be replaced by constant phase elements (*CPE*) [36] to adapt for nonideal behaviour. *CPE* instead of capacitors were actually used in the equivalent circuit models to account for a dispersive character of the time constants and inhomogeneous properties of the layers. *CPE* is marked as *Q* in the circuit description code (CDC) and it is defined by the admittance *Y* and the power index number *n*: $Y = Y_o(jw)^n$. The term *n* shows how far the interface is from an ideal capacitor.

Applying equivalent circuits to fit the impedance spectra a set of fitting parameters was obtained (Table 4). In order to study the corrosion behaviour of the investigated samples impedance spectra were recorded for various immersion times. The EIS diagrams in the Bode format for the FeP/BCe sample exposed to a 0.5 M NaCl solution for the periods from 0.5 to 24 h are presented in Fig. 7.

The variation in the fitting parameters of FeP/B, FeP/BCe, FePCe1/B and FePCe2/B samples versus the immersion time is listed in Table 4. The results obtained demonstrate that after 0.5 h of immersion into a 0.5 M NaCl solution the values of R_{coat} of the investigated FeP/B, FeP/BCe, FePCe1/B, FePCe2/B samples were equal to ~13–20 kΩ cm^2, $n > 0.5$. Here, the sol–gel coating acts mainly as a physical barrier covering the remaining active areas. The addition of cerium as a conversion coating (FePCe1, FePCe2) or as an inhibitor to silane (BCe) significantly improved the charge transfer resistance R_{ct} of the samples (Table 4). FeP/BCe and FePCe1/B, FePCe2/B samples possessed from ~7 to 9-fold higher R_{ct} values, respectively, as compared with those of FeP/B. The FeP samples with Ce1 and Ce2 conversion coatings and additionally with silane (FePCe1/B, FePCe2/B) shows the well-defined third time constant corresponding to the contribution from the intermediate cerium oxide layer (R_{ox}, Q_{ox}). The values of R_{ox} were 11.4 to 17.1 kΩ cm^2.

During the prolongation of immersion time up to 24 h for all the investigated samples R_{coat} decreases to ~0.1–0.2 kΩ cm^2, the coating capacitance Q_{coat} rapidly grows, the values of $n > 0.5$. The increase in immersion time leads to a decrease in the pore resistance of the sol–gel film due to the formation and growth of new cracks and pores. The increase in Q_{coat} may be attributed to hydrolytic degradation of the coating and/or additional water uptake from the electrolyte. The capacitance Q_{coat} of the FeP/BCe sample after 24 h exposure is ~ tenfold lower than that of FeP/B, revealing a higher resistant barrier for the degradation of silane doped with cerium coating.

The evolution of the intermediate cerium oxide layer resistance R_{ox} of the FePCe1/B and FePCe2/B samples has shown the highest initial values of R_{ox}. After 1 h of immersion the values of R_{ox} reach ~1.0 kΩ cm^2 and are stable over 24 h (Table 4). During the 24 h immersion the Q_{ox} parameter is not stable and the evolution of Q_{ox} shows similar capacitance values of the oxide layers of both samples. The increase in Q_{ox} indicates the degradation of the oxide layer during immersion. The capacitance of the sample FePCe2/B has higher values after 1 h of immersion and then drops at a longer immersion time. The factors that can change the capacitance could be the surface area and thickness of the cerium oxide layer. The latter fact of Q_{ox} value variations may be indication of the Ce ion self-healing ability in the multilayer coating. Moreover, in our previous work [33] it was shown that both conversion coatings Ce1 and Ce2 provide an active corrosion protection of carbon steel.

The low frequency part of the impedance spectra can be used to estimate the extent of corrosion activity. The evolution of the charge transfer resistance R_{ct} values is presented in Table 4. With increase in the immersion time R_{ct} values of all the investigated samples show a tendency to

Table 4. **EIS data simulation for the FeP/B, FeP/BCe, FePCe1/B, FePCe2/B samples using equivalent circuits shown in Fig. 7**

Exposure time, h	R_{coat}, kΩ cm²	$Y_0(Q_{coat})\times10^5$, Ω^{-1} cm^{-2} s^n	n (Q_{coat})	R_{ox}, kΩ cm²	$Y_0(Q_{ox})\times10^5$, Ω^{-1} cm^{-2} s^n	n (Q_{ox})	R_{ct}, kΩ cm²	$Y_0(Q_{dl})\times10^5$, Ω^{-1} cm^{-2} s^n	n (Q_{dl})
					FeP/B				
0.5	19.54	2.8	0.58	–	–	–	5.73	0.01	0.99
1	0.37	14.5	0.59	–	–	–	5.7	6.1	0.99
5	0.16	58.1	0.61	–	–	–	2.37	14.3	0.99
24	0.16	140.1	0.64	–	–	–	2.1	32.1	0.99
					FeP/BCe				
0.5	15.0	1.5	0.56	–	–	–	38.8	3.4	0.57
1	6.12	1.9	0.55	–	–	–	34.5	5.0	0.63
5	0.56	6.4	0.54	–	–	–	9.6	9.8	0.61
24	0.11	15.5	0.61	–	–	–	3.83	42.0	0.66
					FePCe1/B				
0.5	13.7	0.8	0.57	11.4	0.8	0.99	39.4	3.5	0.99
1	4.73	6.8	0.55	1.06	0.05	0.99	11.74	0.25	0.99
5	0.35	55.7	0.53	1.1	3.3	0.99	7.7	6.84	0.99
24	0.17	92.2	0.53	0.58	22.1	0.99	4.95	70.2	0.99
					FePCe2/B				
0.5	12.85	0.04	0.80	17.08	0.3	0.99	49.6	5.5	0.99
1	7.98	5.7	0.67	0.8	19.8	0.99	9.87	0.02	0.99
5	0.52	25.6	0.56	0.81	0.08	0.99	4.98	2.1	0.99
24	0.19	41.0	0.57	0.66	6.8	0.99	4.36	17.4	0.99

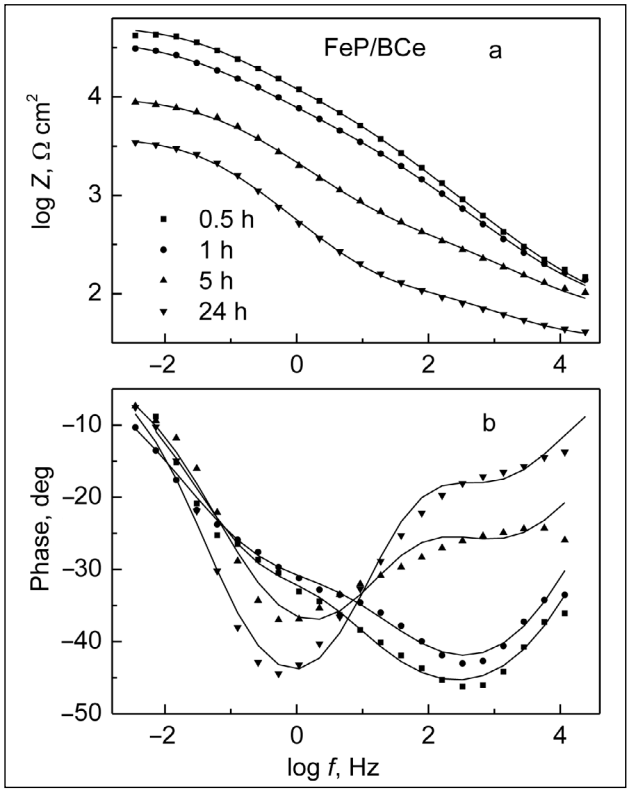

Fig. 7. Bode plots of EIS spectra during immersion of the FeP/BCe sample in a 0.5 M NaCl solution for 24 h

decrease without any signs of recovery. Such changes may indicate that the electrolyte reached the steel substrate. After 24 h of exposure FeP/B has reached the lowest value of R_{ct} = 2.1 kΩ cm², while R_{ct} of the FeP/BCe sample was ~twofold higher. The FePCe1/B and FePCe2/B samples exhibited the highest R_{ct} values equal to 4.95 and 4.36 kΩ cm², respectively. The results obtained imply that after 24 h of exposure the R_{ct} values of FePCe1/B, FePCe2/B and FeP/BCe samples approximated the R_{ct} values of FePCe1 and FePCe2 samples without sol–gel coating [33].

The cerium conversion coatings and the addition of cerium nitrate to silane as an inhibiting agent can certainly help in corrosion protection of carbon steel substrates. The addition of cerium to silane modifies the barrier effect of the coating.

CONCLUSIONS

The investigated multilayer coatings systems on the carbon steel consisted of an amorphous phosphate layer without/with two types of cerium conversion coatings and an additional outer layer of bis-[triethoxysilylpropyl] tetrasulfide (BTESPT) silane, or BTESPT doped with cerium films. The surface morphology and cross-section studies, which were conducted by SEM, revealed that BTESPT films are free of visible defects and cracks. The values of average

thickness of the sol–gel coating on the phosphated carbon steel surfaces without/with cerium coatings did not differ much from each other, as they were 305 and 316 nm, respectively. Meanwhile, the introduction of cerium into the silane coating has caused the reduction in the resulting film thickness up to ~250 nm.

The obtained results of potentiodynamic polarization measurements have revealed that the BTESPT film increased the protection efficiency of all the investigated samples after 0.5 h immersion into a 0.5 M NaCl solution. The calculated values of protection efficiency increased from 80 to 95%. Besides, the phosphated carbon steel samples with the multilayer coatings exhibit better protective abilities with respect to those of the carbon steel samples.

The sol–gel BTESPT coating acts mainly as a physical barrier covering the remaining active areas. The increase of the immersion time leads to the decrease of the pore resistance of the sol–gel film due to formation and growth of new cracks and pores.

The results of EIS measurements performed during 24 h of immersion of the phosphated carbon steel samples into a 0.5 M NaCl solution revealed that the film of BTESPT doped with Ce was more protective than that of the non-modified one. The cerium conversion coatings or the addition of cerium nitrate to BTESPT as an inhibiting agent can certainly help in corrosion protection of carbon steel substrates.

Received 1 September 2017
Accepted 29 September 2017

References

1. B. R. W. Hinton, *Met. Finish.*, **7**, 55 (1991).
2. J. E. Gray, B. Luan, *J. Alloys Compd.*, **336**, 88 (2002).
3. D. B. Freeman, *Phosphating and Metal Pre-Treatment*, Woodhead-Faulkner Ltd., Cambrige, England (1986).
4. D. Weng, P. Jokiel, A. Uebleis, H. Boehni, *Surf. Coat. Technol.*, **88**, 147 (1996).
5. K. Ogle, A. Tomandl, N. Meddahi, M. Wolpers, *Corros. Sci.*, **46**, 979 (2004).
6. A. Tomandl, M. Wolpers, K. Ogle, *Corros. Sci.*, **46**, 997 (2004).
7. Y. K. Song, F. Mansfeld, *Corros. Sci.*, **48**, 154 (2006).
8. C. G. da Silva, I. C. P. Margarit-Mattos, O. R. Mattos, H. Perrot, B. Tribollet, V. Vivier, *Corros. Sci.*, **51**, 151 (2009).
9. A. J. Aldykewicz, H. S. Isaacs, A. J. Davenport, *J. Electrochem. Soc.*, **142**, 3342 (1995).
10. Y. L. Lee, Y. R. Chu, W. C. Li, C. S. Lin, *Corros. Sci.*, **70**, 74 (2013).
11. C. Wang, F. Jiang, F. Wang, *Corros. Sci.*, **46**, 75 (2004).
12. M. Fedel, A. Ahniyaz, L. G. Ecco, F. Deflorian, *Electrochim. Acta*, **131**, 71 (2014).
13. M. A. Arenas, J. J. de Damborenea, *Surf. Coat. Technol.*, **187**, 320 (2004).
14. Y. Kobayashi, Y. Fujiwara, *Electrochim. Acta*, **51**, 4236 (2006).
15. A. Conde, M. A. Arenas, A. de Frutos, J. de Damborenea, *Electrochim. Acta*, **53**, 7760 (2008).
16. X. Yu, G. Li, *J. Alloys Compd.*, **364**, 193 (2004).
17. S. Joshi, E. A. Kulp, W. G. Fahrenholtz, M. J. OʹKeefe, *Corros. Sci.*, **60**, 290 (2012).
18. M. F. Montemor, A. M. Simões, M. J. Carmezim, *Appl. Surf. Sci.*, **253**, 6922 (2007).
19. M. F. Montemor, A. M. Simões, M. G. S. Ferreira, M. J. Carmezim, *Appl. Surf. Sci.*, **254**, 1806 (2008).
20. B. R. W. Hinton, L. Wilson, *Corros. Sci.*, **29**, 967 (1989).
21. R. G. Buchheit, S. B. Mamidipally, P. Schmutz, H. Guan, *Corrosion*, **58(1)**, 3 (2002).
22. D. Guergova, E. Stoyanova, D. Stoychev, I. Avramova, P. Stefanov, *J. Rare Earths*, **33(11)**, 1212 (2015).
23. S. Kiyota, B. Valdez, M. Stoytcheva, R. Zlatev, J. M. Bastidas, *J. Rare Earths*, **29(10)**, 961 (2011).
24. B. Valdez, S. Kiyota, M. Stoytcheva, R. Zlatev, J. M. Bastidas, *Corros. Sci.*, **87**, 141 (2014).
25. D. R. Arnott, B. R. W. Hinton, N. E. Ryan, *Corrosion*, **45**, 12 (1989).
26. D. Wang, G. P. Bierwagen, *Prog. Org. Coat.*, **39**, 67 (2009).
27. W. Trabelsi, E. Triki, L. Dhouibi, M. G. S. Ferreira, M. L. Zheludkevich, M. F. Montemor, *Surf. Coat. Technol.*, **200**, 4240 (2006).
28. M. F. Montemor, W. Trabelsi, S. V. Lamaka, K. Y. Yasakau, M. L. Zheludkevich, A. C. Bastos, M. G. S. Ferreira, *Electrochim. Acta*, **53**, 5913 (2008).
29. I. Santana, A. Pepe, E. Jimenez-Pique, S. Ceré, *Surf. Coat. Technol.*, **236**, 476 (2013).
30. F. Schreiber, *Prog. Surf. Sci.*, **65**, 151 (2000).
31. L. S. Kasten, J. T. Grant, N. Grebasch, N. Voevodin, F. E. Arnold, M. S. Donley, *Surf. Coat. Technol.*, **140**, 11 (2001).
32. B. A. Boukamp, *J. Electrochem. Soc.*, **142**, 1885 (1995).
33. O. Girčienė, L. Gudavičiūtė, A. Selskis, V. Jasulaitienė, S. Šakirzanovas, R. Ramanauskas, *Chemija*, **26(3)**, 175 (2015).
34. K. A. Yasakau, J. Carneiro, M. L. Zheludkevich, M. G. S. Ferreira, *Surf. Coat. Technol.*, **246**, 6 (2014).
35. M. L. Zheludkevich, R. Serra, M. F. Montemor, K. Y. Yasakau, I. M. Miranda Salvado, M. G. S. Ferreira, *Electrochim. Acta*, **51**, 208 (2005).
36. K. Jütnerr, *Electrochim. Acta*, **35**, 1501 (1990).

O. Girčienė, L. Gudavičiūtė, A. Martušienė, A. Selskis, V. Jasulaitienė, R. Ramanauskas

BIS-[TRIETOKSISILILPROPIL] TETRASULFIDO SILANO DANGŲ ĮTAKOS ANGLINIO PLIENO APSAUGAI NUO KOROZIJOS TYRIMAS

S a n t r a u k a

Darbo tikslas – ištirti zolio-gelio bis-[triethoxysilylpropyl] tetrasulfide (BTESPT) dangos įtaką anglinio plieno koroziniam atsparumui 0,5 M NaCl tirpale. Ištirti anglinio plieno ir fosfatuoto anglinio plieno (be/su cerio konversinėmis dangomis) bei papildomai padengti sluoksniu BTESPT ar BTESPT, praturtinto cerio druska, pavyzdžiai. Pasirinktų pavyzdžių cheminė sudėtis bei struktūra tirti SEM ir XPS metodais, o korozinė elgsena nustatyta atliekant elektrocheminius tyrimus (voltamperometrijos ir EIS). Gauti tyrimų duomenys parodė, kad geresnėmis antikorozinėmis savybėmis pasižymi fosfatuoto plieno su cerio konversinėmis dangomis ir zolio-gelio sluoksniu bei fosfatuoto plieno, kuris padengtas BTESPT, praturtinto cerio sluoksniu, pavyzdžiai. Nustatyta, kad cerio konversinės dangos ir sluoksnis BTESPT, praturtintas cerio nitratu, kuris yra korozijos inhibitorius, padidina anglinio plieno apsaugą nuo korozijos.